Processing Ocean-Bottom Seismic (OBS) Data from the White Rose oilfield, offshore Newfoundland

Peter W. Cary and Robert R. Stewart

ABSTRACT

A four-component ocean-bottom seismometer (OBS) survey was acquired over the White Rose oilfield, offshore Newfoundland in the summer of 2002. The survey consisted of 21 OBS units (normally used in crustal refraction experiments) deployed over 1 km with 12 sources lines from a towed air gun. There were numerous problems with the data, but some promising final sections were achieved for both PP waves (largely on the vertical channel) and PS waves (mainly on the radial channel). Processes applied to the data included data clipping repair, F-K and tau-p filtering, PP and PS stacking, and post-stack migration. Final images indicate considerable promise for multicomponent marine data in this area.

INTRODUCTION

The White Rose oilfield, offshore Newfoundland has considerable hydrocarbon reserves as well as significant seismic imaging challenges. In attempting to solve some of these seismic problems in the area, we have proposed ocean-bottom seismic measurements. However, as four-component ocean-bottom cable (OBC) acquisition is untried on the East Coast of Canada and quite expensive, this promising measurement has not yet been undertaken. Nonetheless, Dalhousie University has been conducting ocean-bottom seismometer (OBS) surveys for crustal refraction purposes for some time (Figure 1). Using several shot gathers from a deep deployment in the summer 2000 cruise of the Dalhousie OBS, we processed them to see if there was any reflection energy apparent. To our delight, there appeared to be energy on both the vertical and radial geophones. With these encouraging results, we proposed and shot a test survey over the White Rose oilfield using the Dalhousie OBS.

This report describes the processing of the four-component ocean-bottom seismic data that was acquired in May/June of 2002 by Dalhousie University in collaboration with the CREWES Project at University of Calgary and Husky Energy Inc. The acquisition was performed with Dalhousie's ocean bottom seismometers (OBS). These instruments (Figure 1) have been used in previous cruises primarily for deep crustal seismological research. Specific details about these instruments can be found at http://www.phys.ocean.dal.ca/seismic.

The Dalhousie OBS instruments had not previously been used for this type of shallow crustal exploration study, so one of the concerns before the data were acquired was whether these instruments would perform well in these conditions. Some severe problems did occur with the quality of the data that was acquired. Several different undesirable and sometimes overwhelming types of noise are present on the recorded data. Much of this report is concerned with the identification and description of these types of noise, and with the methods that were used to try to attenuate them.

The data processing was somewhat compromised by the noisiness of the data. Nevertheless, the quality of the final stacks turned out to be surprisingly good. It appears that the most reliable image was obtained from the vertical component of the geophone on its own, without combination with the hydrophone data. The horizontal components of the geophone show strong converted-wave reflections. This study has clearly shown that high-quality images are attainable with marine multicomponent OBS data off the east coast of Canada.

ACQUISITION AND GEOMETRY

A total of 21 OBS instruments were available for acquisition, so they were laid out in a 2D line along the ocean floor approximately 50m apart in order to form a 1 km east-west line of receivers. The OBS instruments were dropped over the side of the ship and drifted to the bottom through approximately 125m of water. Once these receivers were laid out, a series of 12 east-west source lines were acquired with a 1966 cu. in., 1650-1800 psi, 5 airgun array. The source interval was 50m and the source line interval varied from 50m to 200m. Figure 2 shows the location of shot lines along with the approximate location of the 21 OBS receivers. The shot lines appear more crooked than they really are because of the vertical exaggeration of the plot. The real dimensions of the plot are about 1500m (N-S) by 8000m (E-W).

FIG. 1. Dalhousie ocean bottom seismometer (OBS). Picture taken from Dalhousie Seismic Group website (www.phys.ocean.dal.ca/seismic/)

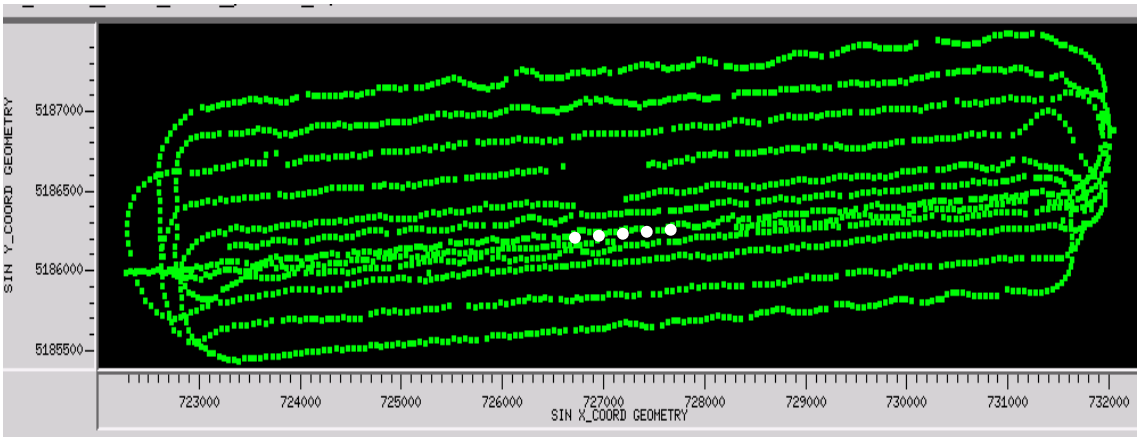

FIG. 2. Location of source lines (green) and approximate position of 21 OBS receivers. The dimensions of the plot are about 1500m in the N-S direction and about 8000m in the E-W direction.

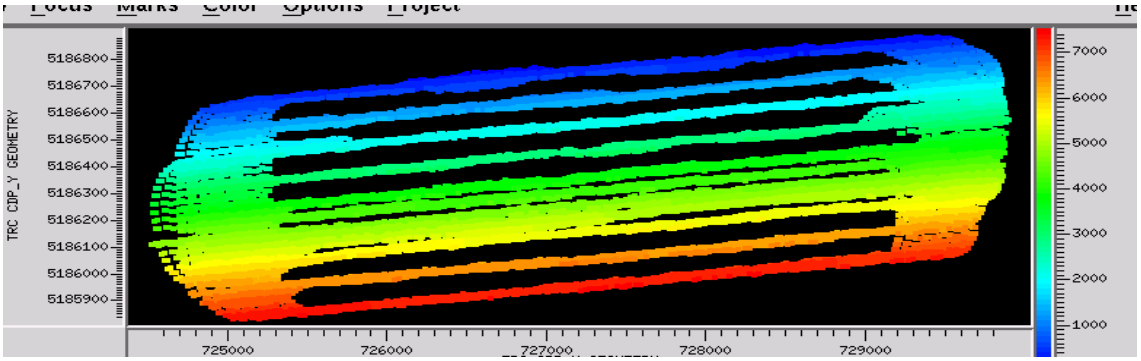

FIG. 3. Midpoint scatter plot. Note the gaps in coverage.

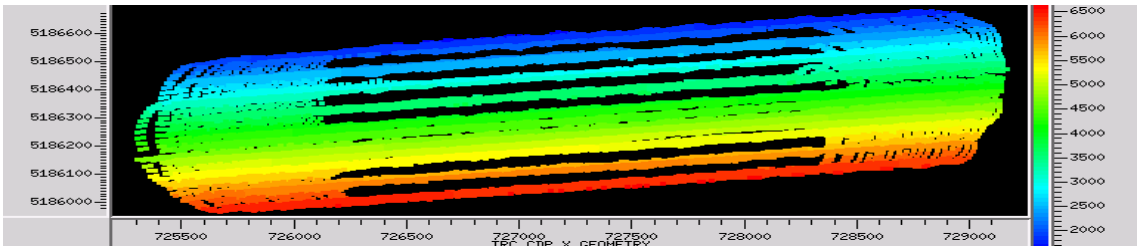

FIG. 4. Asymptotic conversion points for Vp/Vs = 2.05. Notice that the lines closer to the receivers than for the midpoint map.

Figure 3 shows the midpoint locations of all traces in the survey, and Figure 4 shows the asymptotic CCP positions for the P-S data with Vp/Vs = 2.05. The data were sorted into 25m x 25m cdp bins. The cdp grid has 35 inlines running in the east-west direction and 216 crosslines running in the north-south direction. A nominal fold of about 12 was obtained along 12 of the inlines (one inline for each of the 12 source lines). A large number of empty bins exist between each of these 12 inlines. The goal was to process all source lines together as a sparse 3D survey in order to allow a 3D migration of the data, so interpolation of the data into neighbouring bins was necessary. The details of this interpolation are included later in this report.

LOCATION OF RECEIVERS

The OBS instruments were simply dropped over the side of the ship and drifted down through about 125m of water to the ocean bottom. The positions of the drop points were known from GPS, and the final resting places of the OBS's were calculated using a method that minimized the difference between the actual and predicted first-break times, assuming a constant water velocity of 1500m/s through the water column.

Figure 5 shows the vectors pointing from the drop points to the predicted positions for the 20 receivers. Notice that OBS 3 is missing since it failed to record any signal whatsoever. The vectors in Figure 5 are too small to see clearly, so Figure 6 is included to show some of the receiver line in more detail. We can see that the instruments generally moved south from the drop points, drifting anywhere from 10 to 20m to their final positions on the sea floor.

DATA POLARITY

The polarity of the data for all components during the processing was kept the same as the recorded polarity. It was assumed that the three elements of the geophone formed a righthanded coordinate system. If that is false (i.e. if it is lefthanded instead of righthanded), the effect would be that the actual azimuth angles used in rotating into radial and transverse coordinates would be opposite to those used in processing.

FIG. 5. Displacement vector from the OBS drop points to their predicted positions on the sea floor.

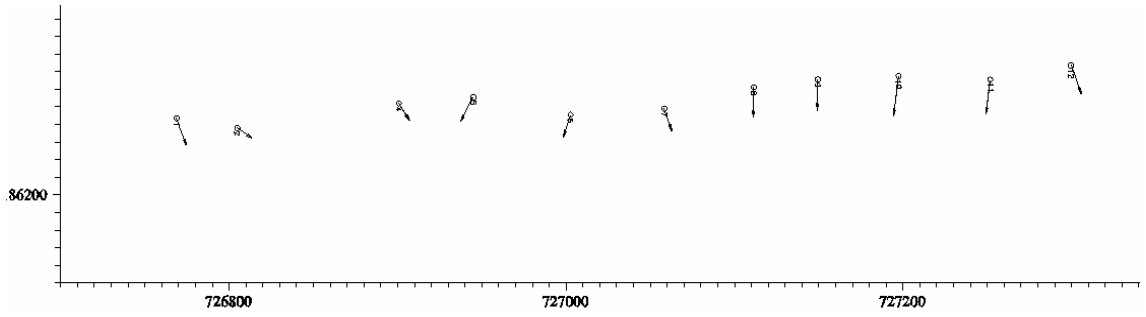

FIG. 6. Close-up of west end of displacement vectors in Figure 5.

PRESTACK DATA QUALITY

The quality of data, when it first was examined, was difficult to understand because it was so variable from receiver to receiver. To give an impression of the variability of the prestack data, Figures 7, 8 and 9 are included. These figures show portions of receiver gathers for OBS 201, 204 and 212. There are four parts to each figure: (a) hydrophone, (b) vertical geophone, (c) horizontal geophone component 1, and (d) horizontal geophone component 2. For example, Figure 7(a) shows the first two source sail lines recorded by the hydrophone of OBS 1, at the west end of the receiver line. A 1000ms AGC has been applied to all traces. 12 seconds were recorded, but only 6 seconds are displayed. The sample rate is 1.792ms. The maximum offset on these records is about 4 km.

On prestack records the hydrophone component has the strongest reflections compared to the other components. For example, notice the strong reflected energy in Figure 7(a) starting at about 2.2s two-way time. This strong reflection marks the bottom of Tertiary sediments, a prominent geologic marker in this area. Note the periodicity of the reflections that follow, with a period of about 167ms. These are strong multiples of the primary event reverberating in the water column. The Whiterose area is well known to have a hard water bottom, which gives difficulties in imaging conventional streamer data.

These same events are also visible in Figure 8(a), however they are partially obscured by some low-frequency noise that appears on all traces. This low-frequency noise problem occurs to a varying degree on all records, but its intensity is receiver consistent. Figure 7(a) and 8(a) also show a problem of amplitudes going off-scale (bit saturation) on near-offset hydrophone traces. The recording system used only 16 bits, and there was some difficulty in knowing how to correctly set the amplitude gain factor on the instruments. These traces had to be surgically muted out of the dataset.

Figure 9(a) should presumably look similar in character to Figure 7(a) and 8(a), but it obviously does not. There actually is good data on this hydrophone record, but it is contaminated by a large amount of high-frequency noise for some reason. It does not affect the geophone records for the same OBS. Inconsistencies in the data quality such as this made it difficult to combine the data from the entire dataset in a reliable fashion. For example, even the polarity of the first breaks on this noisy of a record is difficult to determine.

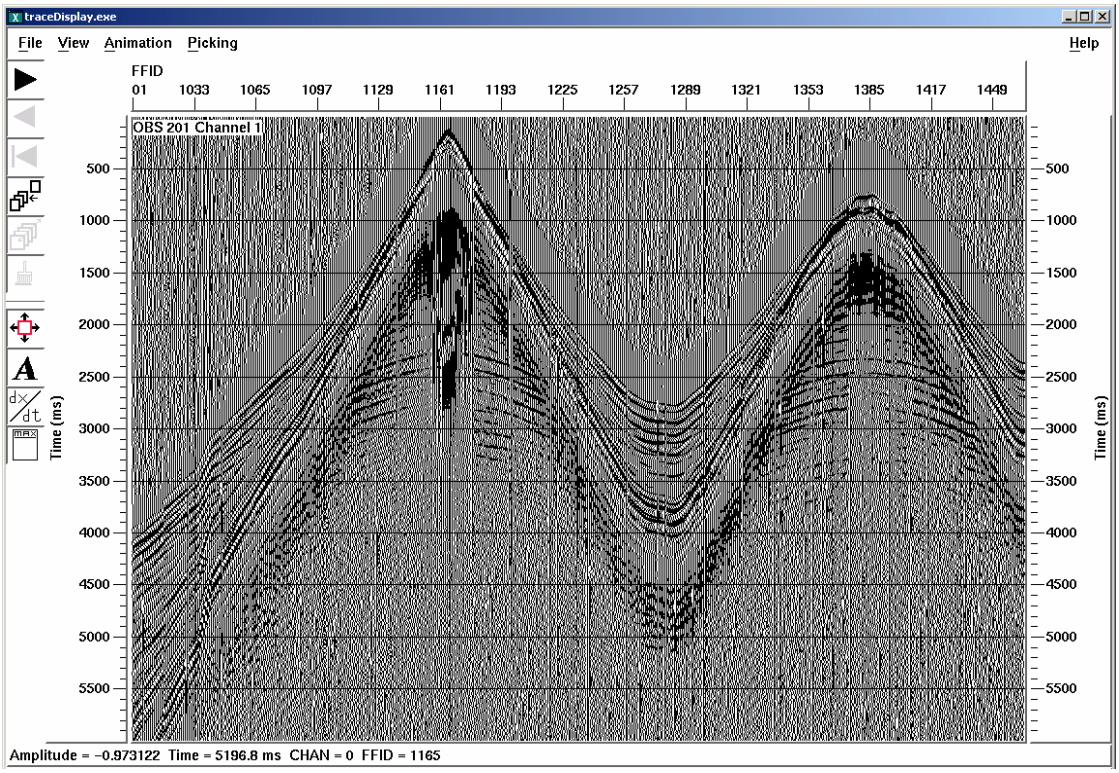

FIG. 7(a). Hydrophone component. First 2 sail lines of common receiver gather (OBS 201).

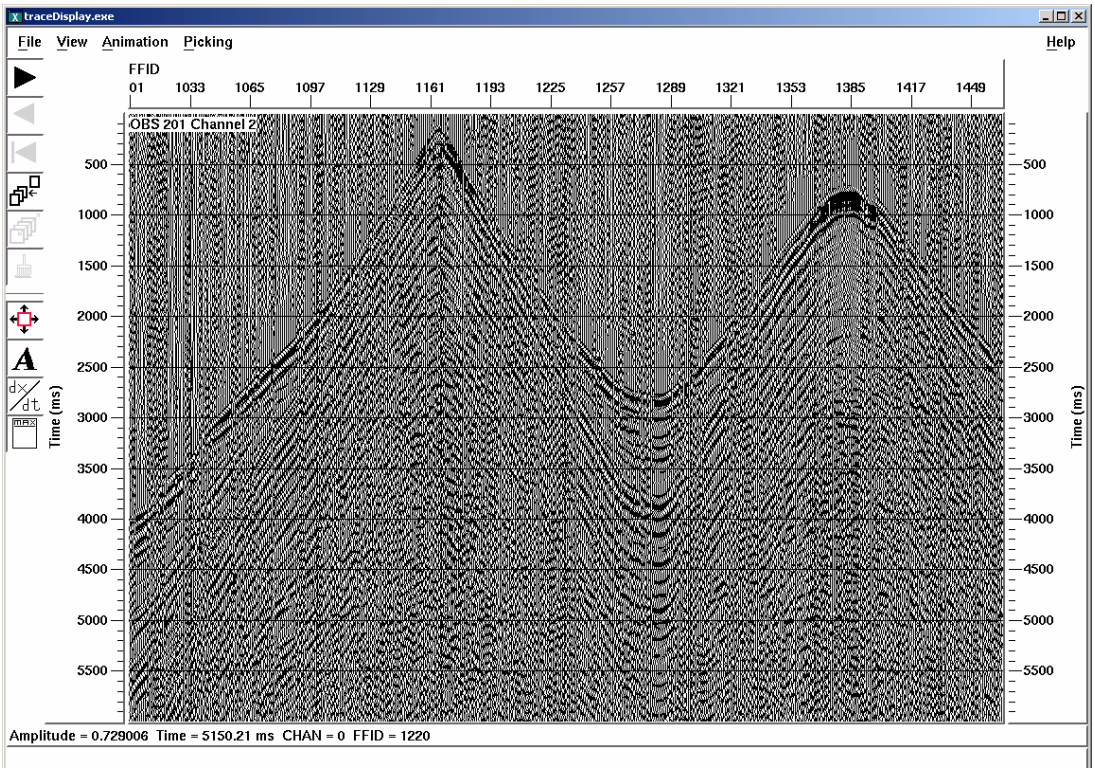

FIG. 7(b). Vertical geophone component. First 2 sail lines of common receiver gather (OBS 201).

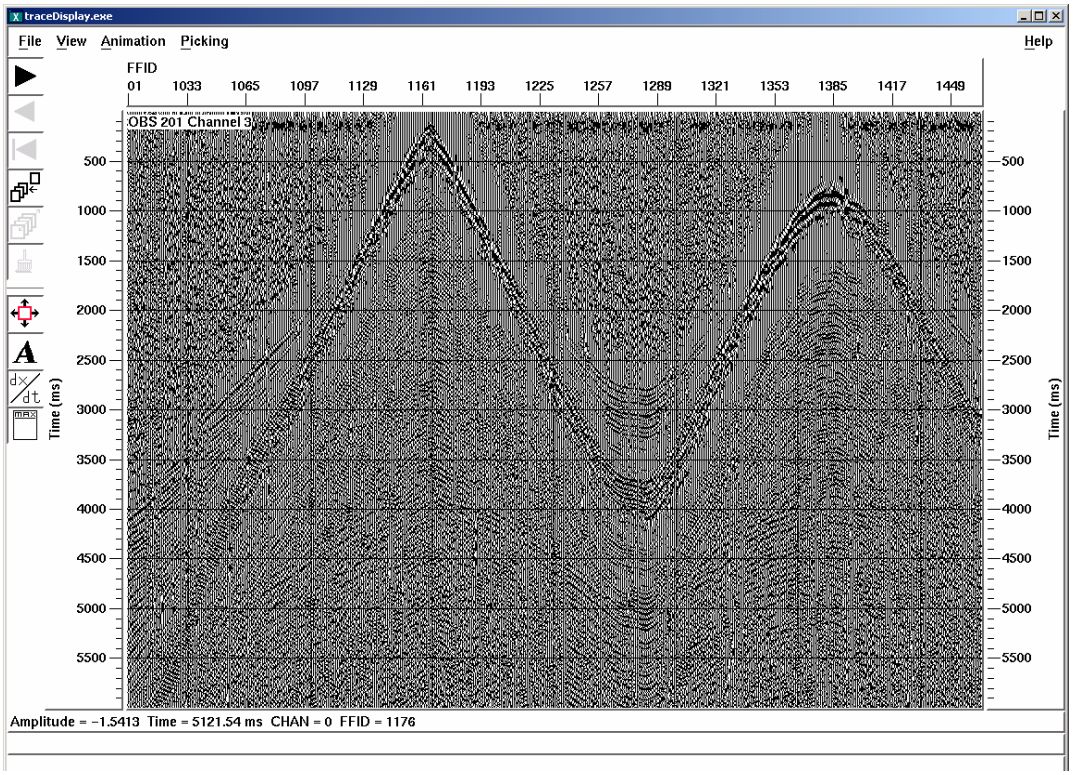

FIG. 7(c). First horizontal geophone component. First 2 sail lines of common receiver gather (OBS 201).

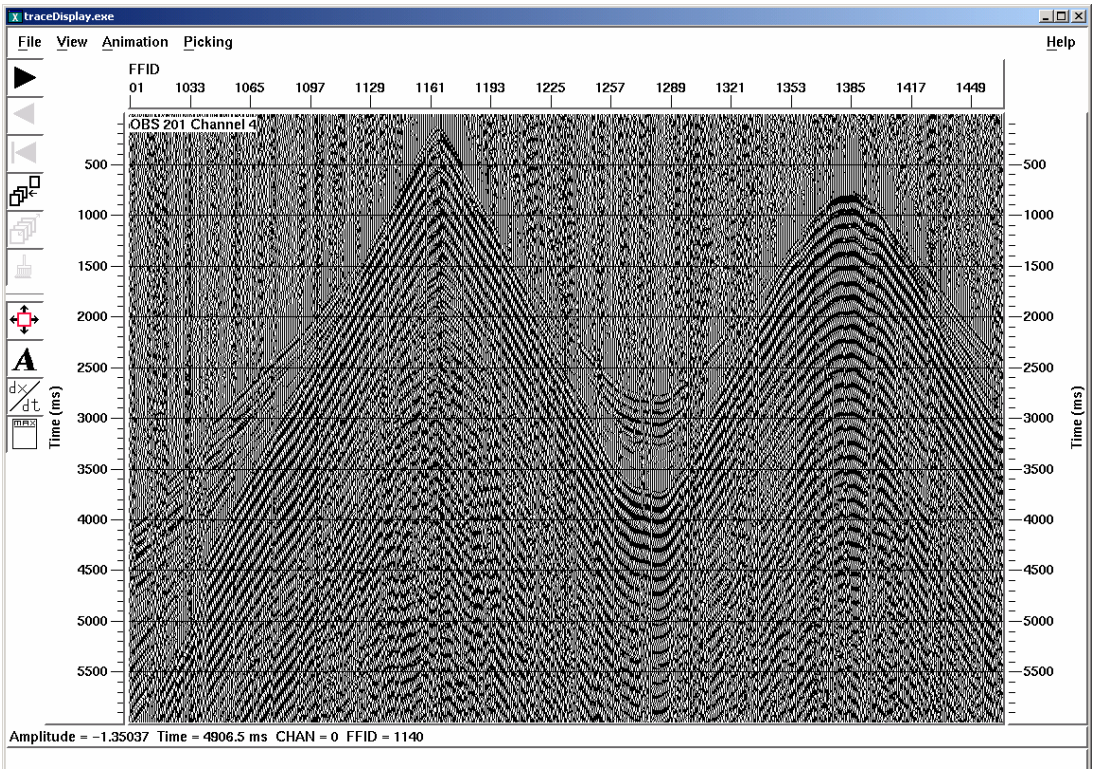

FIG. 7(d). Second horizontal geophone component. First 2 sail lines of common receiver gather (OBS 201).

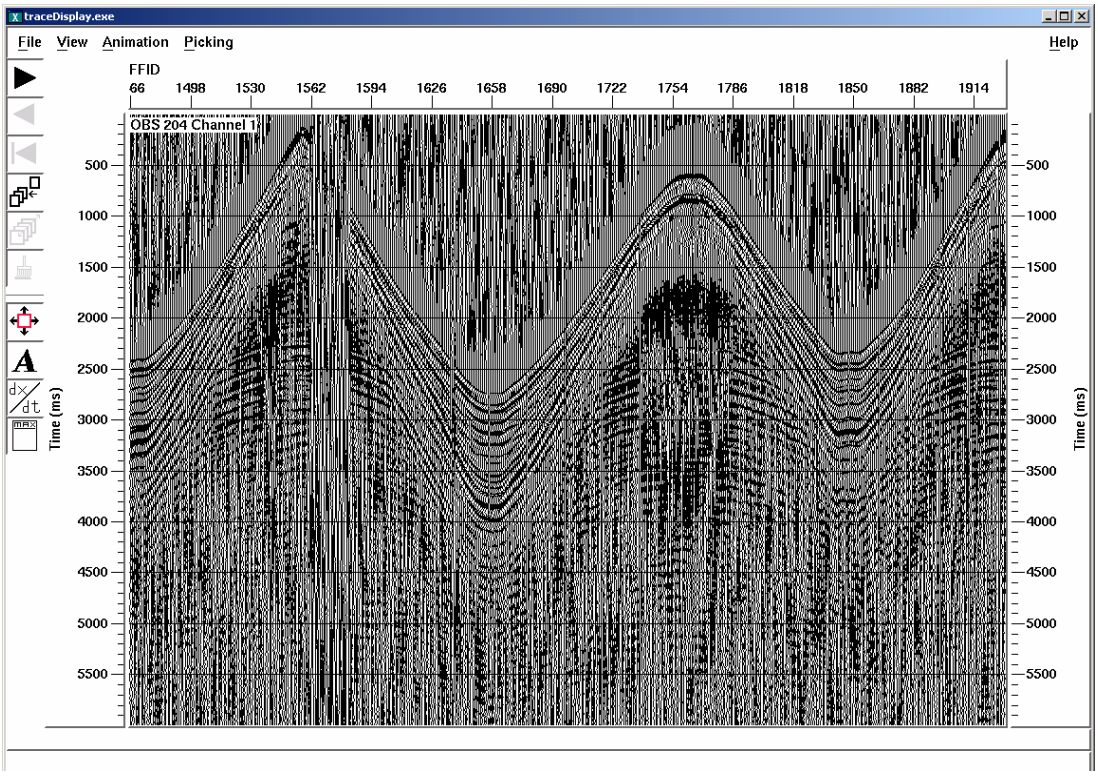

FIG. 8(a). Hydrophone component. First 2 sail lines of common receiver gather (OBS 204).

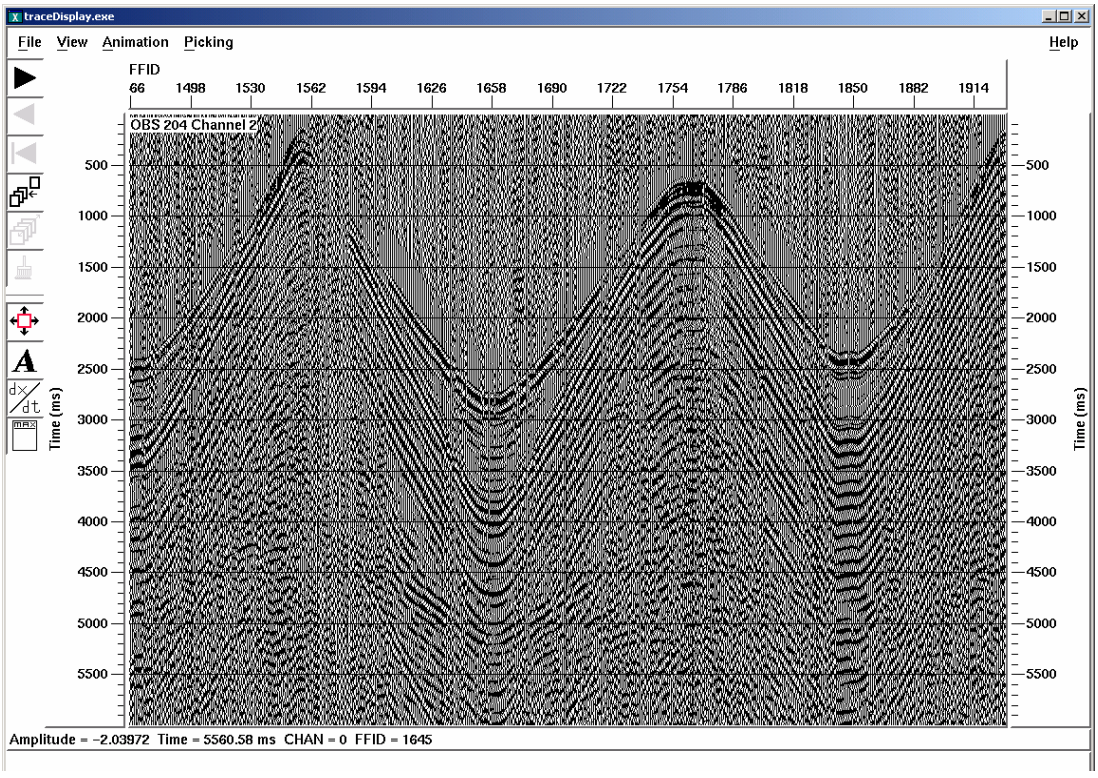

FIG. 8(b). Vertical geophone component. First 2 sail lines of common receiver gather (OBS 204).

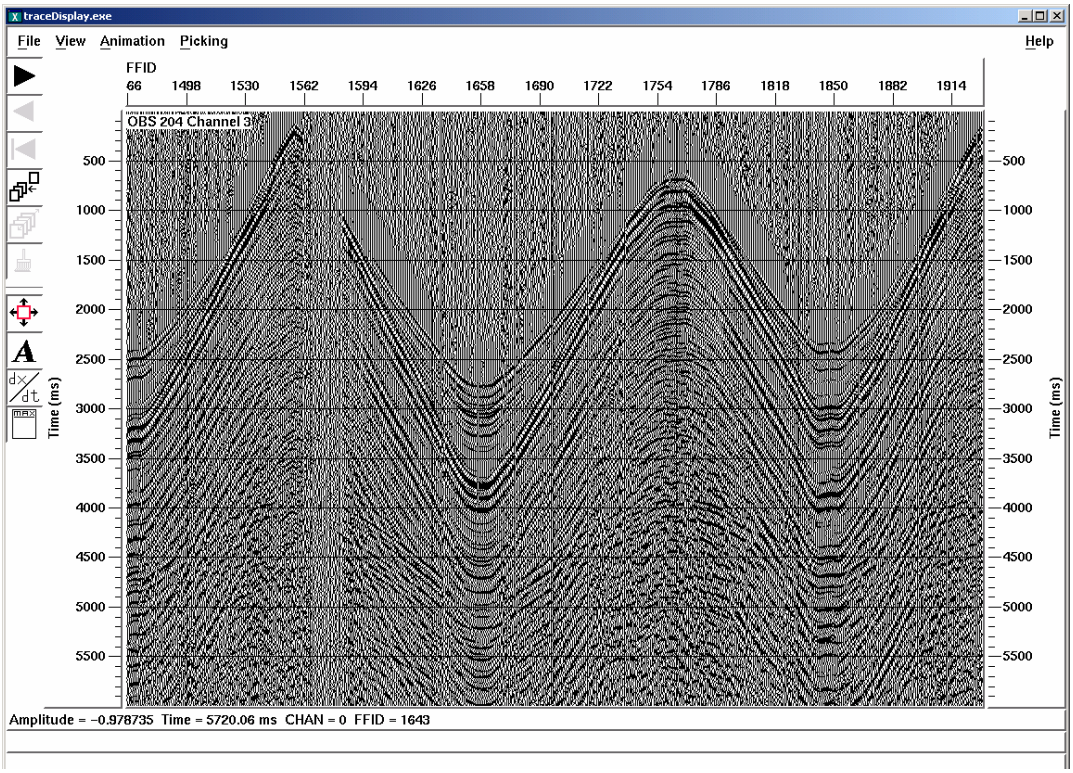

FIG. 8(c). First horizontal geophone component. First 2 sail lines of common receiver gather (OBS 204).

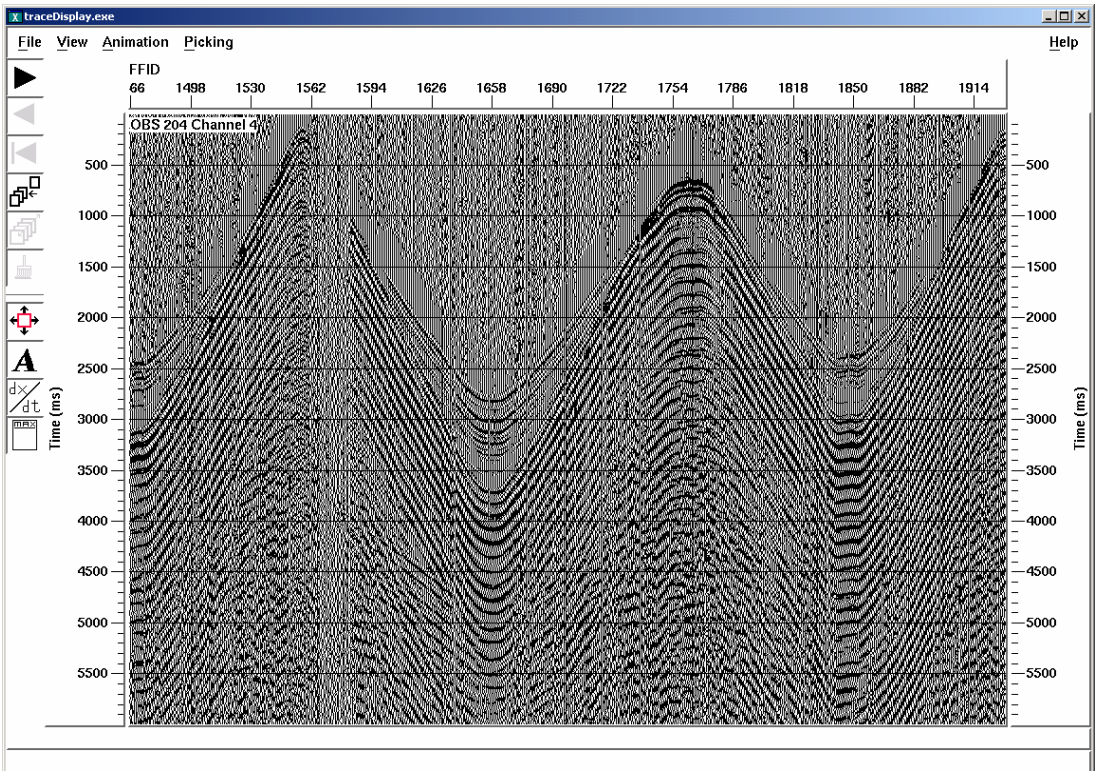

FIG. 8(d). Second horizontal geophone component. First 2 sail lines of common receiver gather (OBS 204).

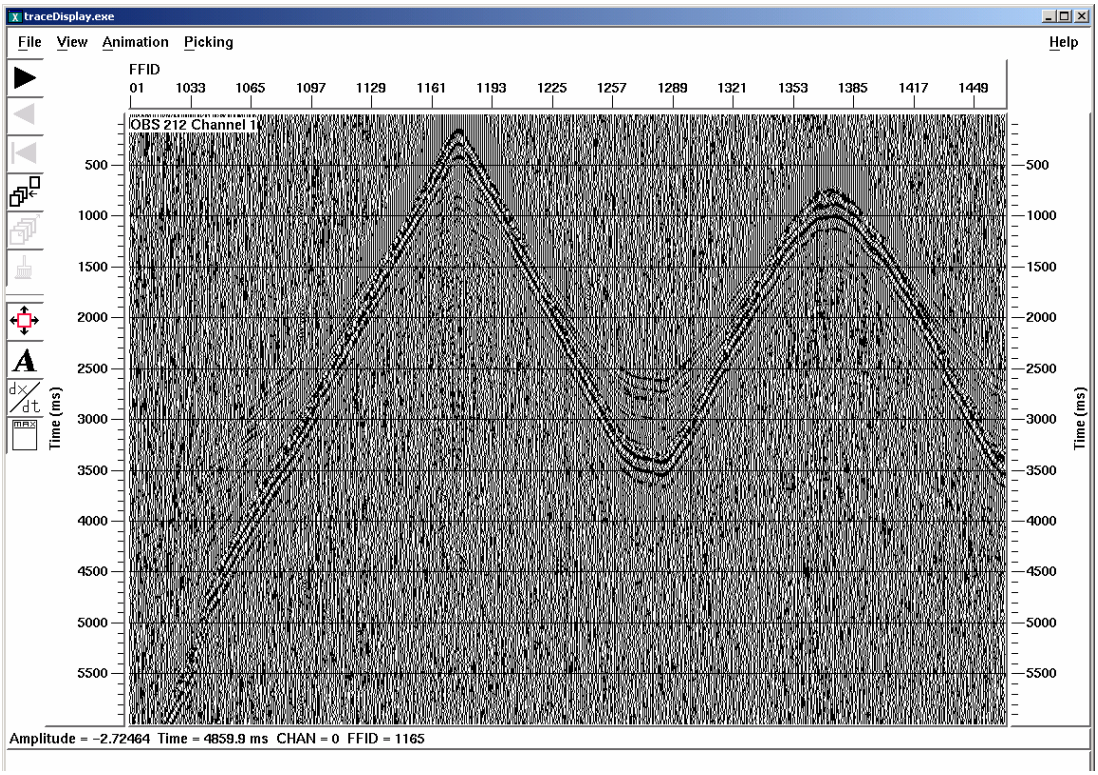

FIG 9(a). Hydrophone component. First 2 sail lines of common receiver gather (OBS 212).

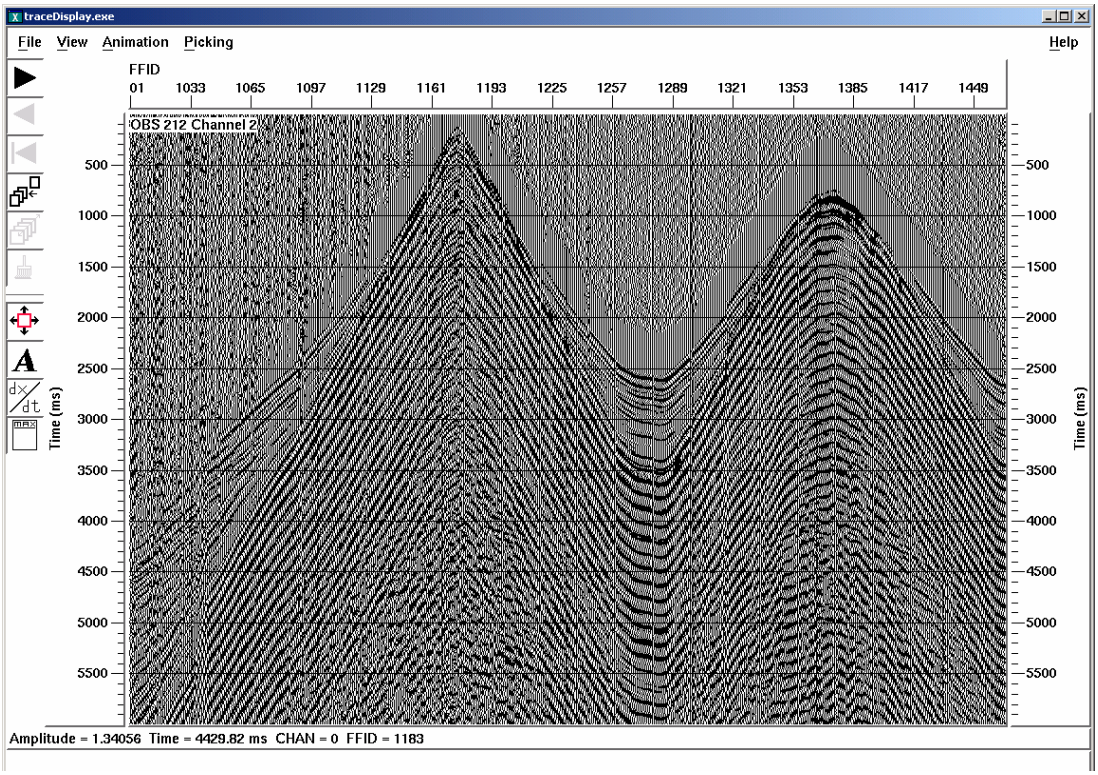

FIG. 9(b). Vertical geophone component. First 2 sail lines of common receiver gather (OBS 212).

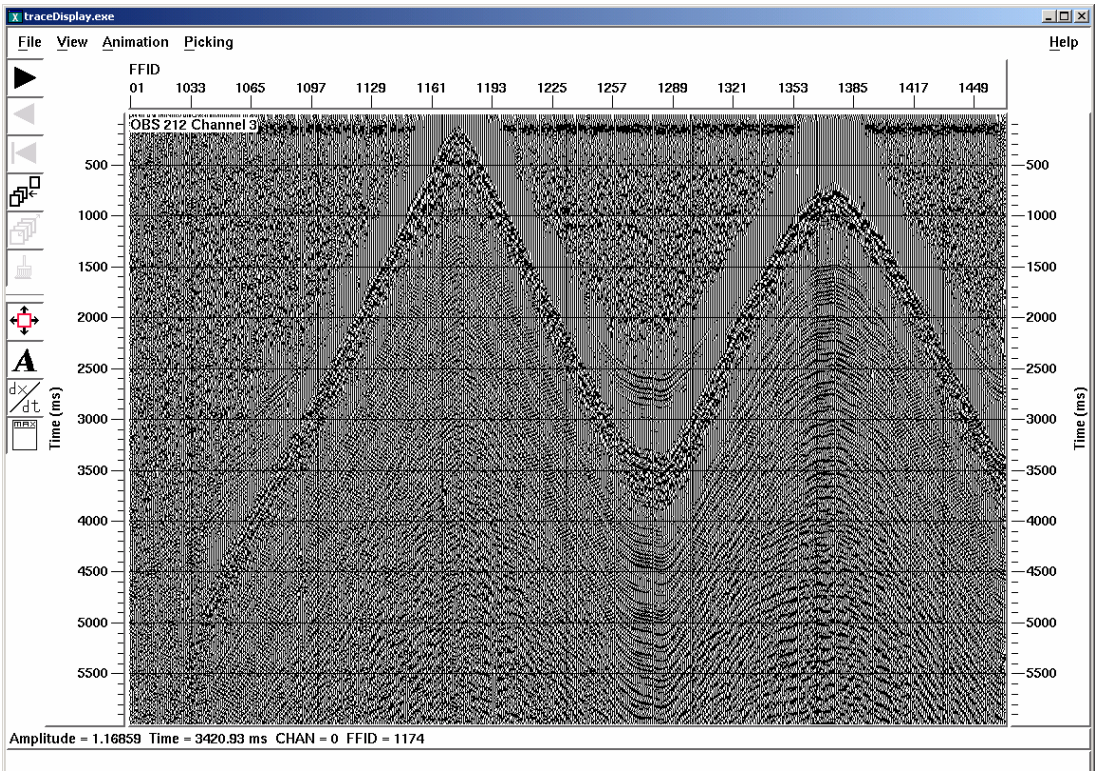

FIG. 9(c). First horizontal geophone component. First 2 sail lines of common receiver gather (OBS 212).

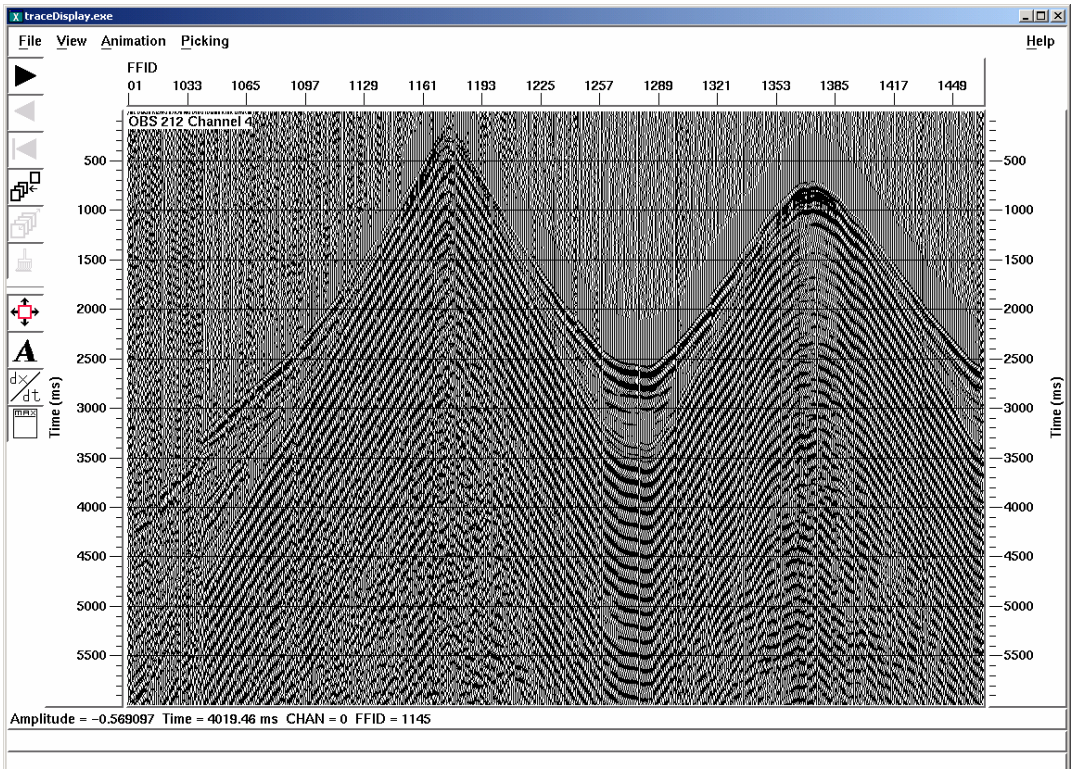

FIG. 9(d). Second horizontal geophone component. First 2 sail lines of common receiver gather (OBS 212).

DATA CLIPPING PROBLEM

A problem with "clipping" of some of the data samples near the first breaks is seen in Figure 10. Presumably this problem was caused by the sign bit in the 16-bit recording system being over-written. Some software that was specifically designed to fix this problem was written, and as Figure 10 illustrates, it is successful at fixing the problem, as long as it was not too severe.

ANTIALIAS FILTERING

Examination of the receiver gathers for all components, revealed that five OBS's yielded data with much more high-frequency noise than others. It was initially thought that this was just a scaling problem. Then it was determined that the first breaks for these five receivers were all about 45ms early compared to the others. It was eventually determined that a fundamental problem had inadvertently occurred during the recording of the data.

Figure 11 shows portions of "noisy" and "clean" hydrophone receiver gathers along with their amplitude spectra. It is clear that an abrupt truncation of the high frequencies is present on the "clean" data. Although this was never confirmed to be true, it appears that an optional high-cut antialias filter (25Hz high cut) was turned on for 15 of the 20 OBS instruments. The nearest offsets of all the hydrophone receiver gathers are shown in Figure 12. It is clear from the noise levels, as well as from the first break arrival times, which instruments had the antialias filter turned on or off.

Ironically, the unintentional application of the 25Hz antialias filter may have led to better recorded data since the data from the OBS instruments without the antialias filter are all too high in amplitude, apparently saturating the 16 bit instruments. In this case it was a matter of luck that two wrongs (antialias filtering and incorrect gain) made a right, or at least a partial right. Nevertheless, it is unfortunate that the final images essentially contain no reliable energy above 25Hz. No high-cut filter was applied in the processing, but there was little energy above 25Hz to preserve. With the advantage of hindsight, it appears that higher frequencies could be recorded and processed from this area with proper instrumentation.

Additional Noise Problems

In addition to the antialias problem already mentioned, a few other problems are present in the data. Figures 13 and 14 show the power spectra of a vertical component and a horizontal component of one OBS. A periodicity in the appearance of notches and peaks in the spectra is to be expected due to the receiver-side ghost. The water depth is 125m, so the separation between primary and ghost arrivals at the geophone is 167ms. This implies that the separation between notches in the power spectra is 6Hz, which is evident in Figures 13 and 14.

In addition to these features, however, there is a spurious peak at about 8.5Hz on these two records, and this peak is present on many other records as well. The origin of this noise is unknown. Attempts to use a sinusoidal noise removal method that is designed for powerline noise were unsuccessful, presumably due to some temporal variation in the

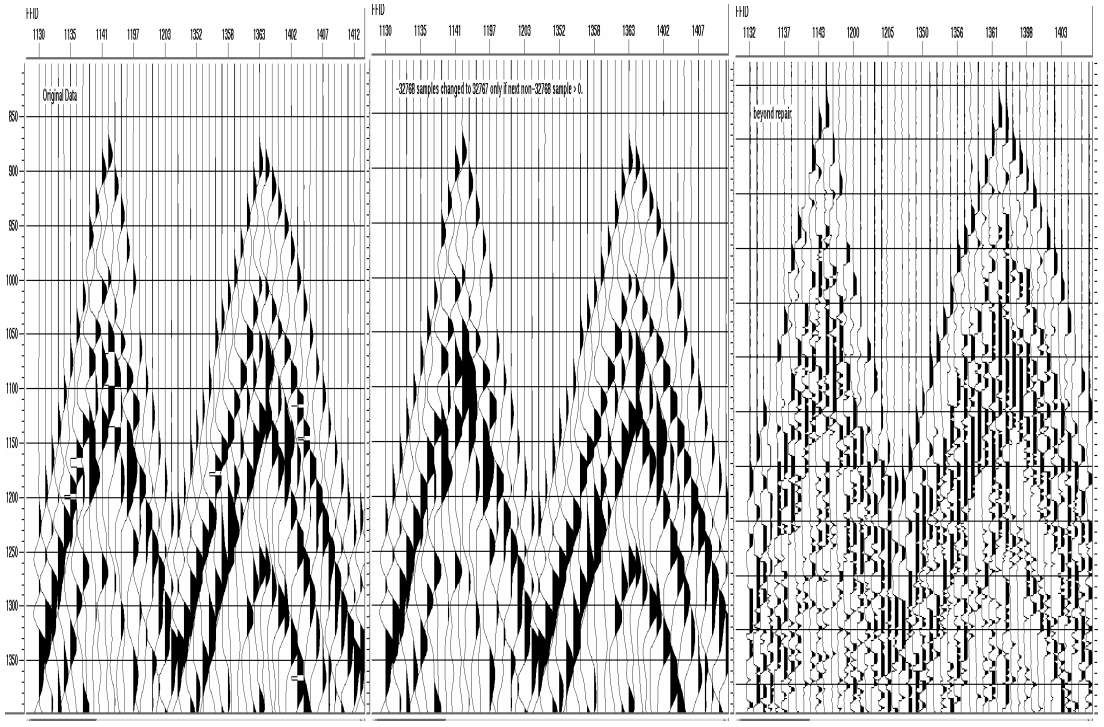

FIG. 10. Data clipping problem before and after repair, as well as one example that is beyond repair.

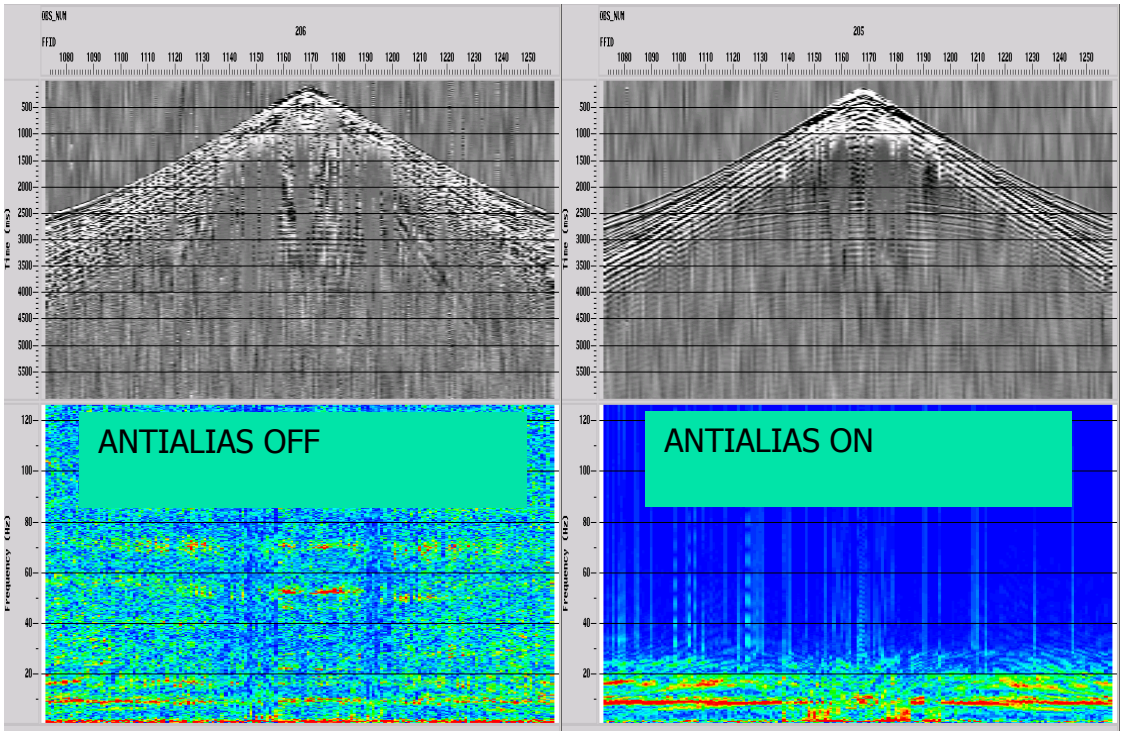

FIG. 11. Noisy gather (left) and clean gather (right) along with their amplitude spectra. The frequencies above 25Hz were not recorded on 15 of the 20 OBS's because of an antialias filter applied during the recording.

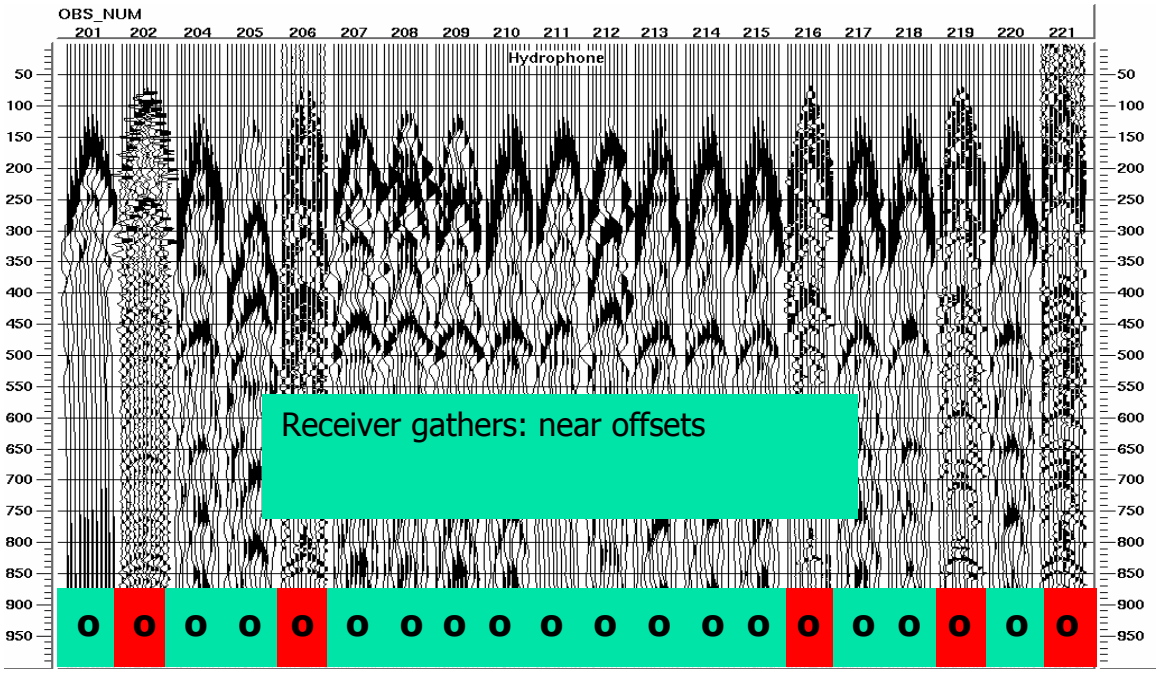

FIG. 12. Nearest offsets of all receiver gathers. Notice that the first breaks of OBS's marked with o's on a red background are earlier than the rest and that they have higher frequency content. These OBS's had an internal antialias filter turned off while the others had it on. Notice that OBS's 205 and 212 appear to be opposite in polarity compared to the others.

noise. A notch filter was used instead, but it was applied selectively to those traces whose peak frequency lies between 7Hz and 10Hz.

In addition, the peak at very low frequencies, below 4Hz should not be there. This low frequency problem is more evident on some records than others (for example Figure 7(a)). It was decided to apply a low cut filter (4-8-279-279Hz) after deconvolution in order to eliminate this noise. Figure 15 illustrates the effect on one receiver gather.

The most serious problem of all was caused by the reverberation noise that is observed in the data in Figure 16. This noise is parallel to the first breaks and rings through the records for far longer than it should, if it were due to multiples. In general the water column multiples (with a period of about 167ms) are expected to be the highest amplitude, and slowest decaying, on the hydrophone component. However, this reverberatory noise is present only on the geophone components, and not on the hydrophones. It is therefore probably due to some sort of resonance in the geophones or in the way that they are attached to the structure.

Figure 16 shows the result of applying an F-K filter to this data, which was found to be the most successful method for removing the noise. It was certainly not entirely successful, but it was better to apply this filter before deconvolution than to let the deconvolution try to attenuate this noise on its own.

As a final note, it was found to be necessary to reverse the polarity of 2 hydrophone receivers and 3 vertical component receivers.

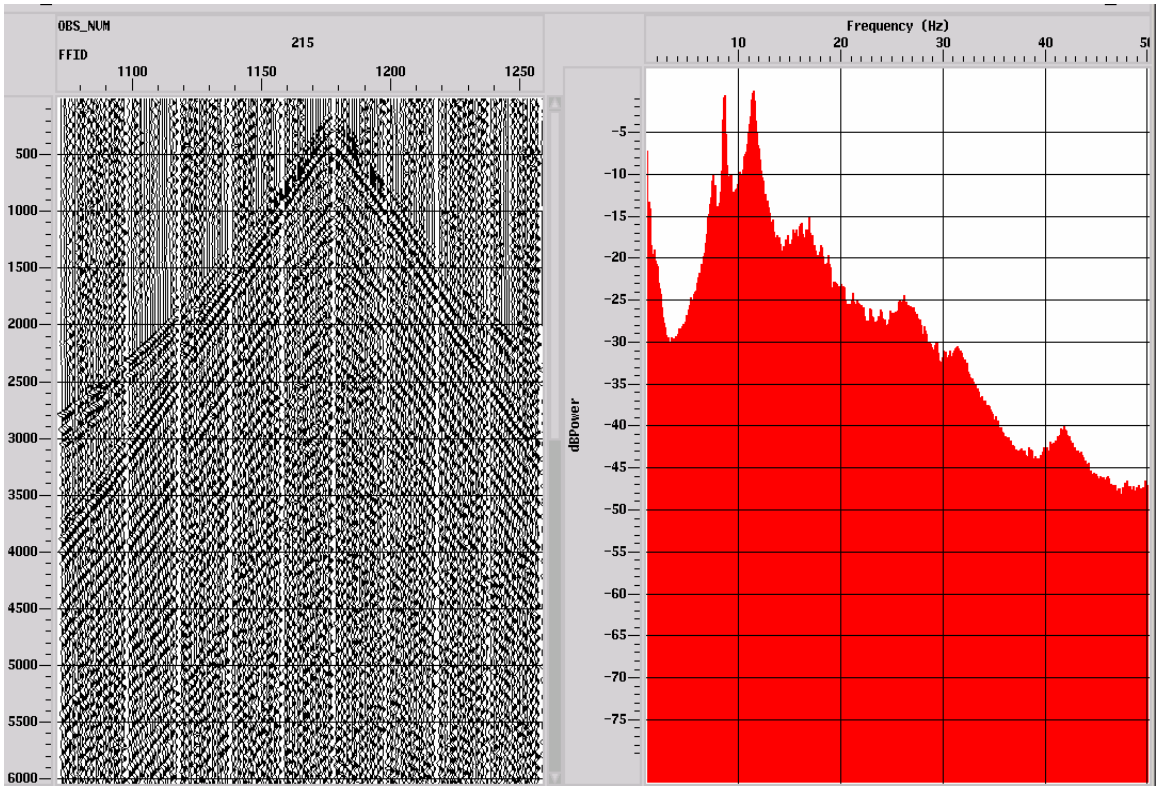

FIG. 13. Vertical geophone component traces and average power spectrum

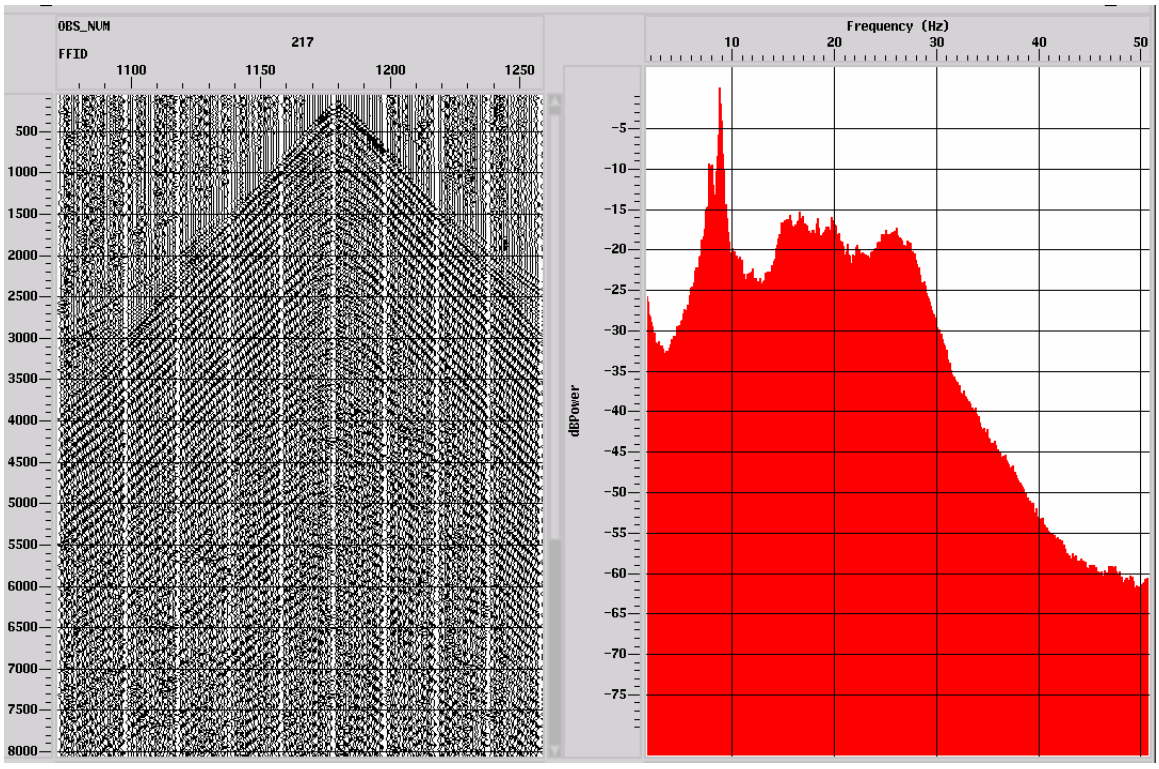

FIG. 14. Horizontal geophone component traces and average power spectrum.

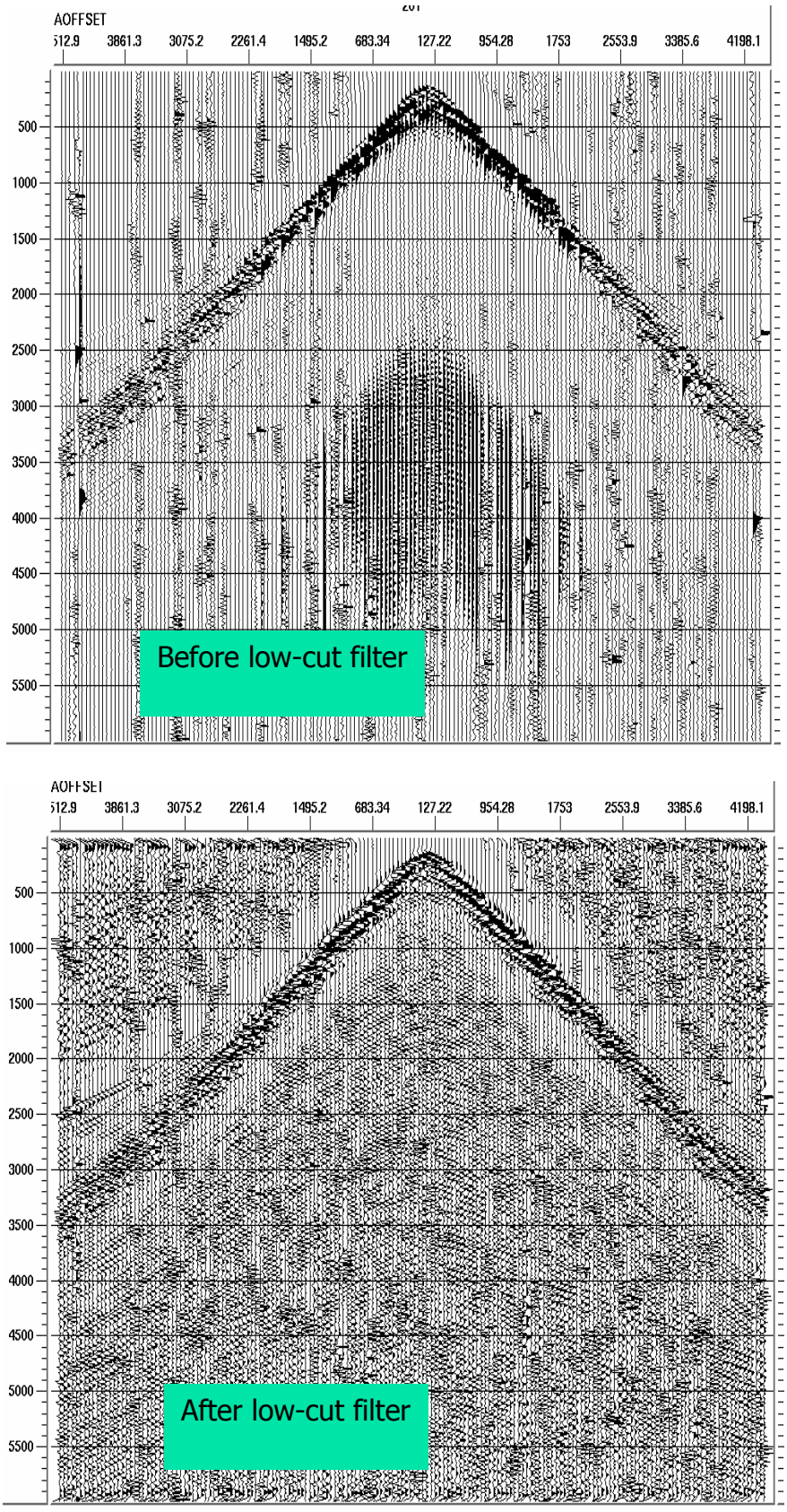

FIG. 15. Hydrophone gather before and after application of low-cut filter.

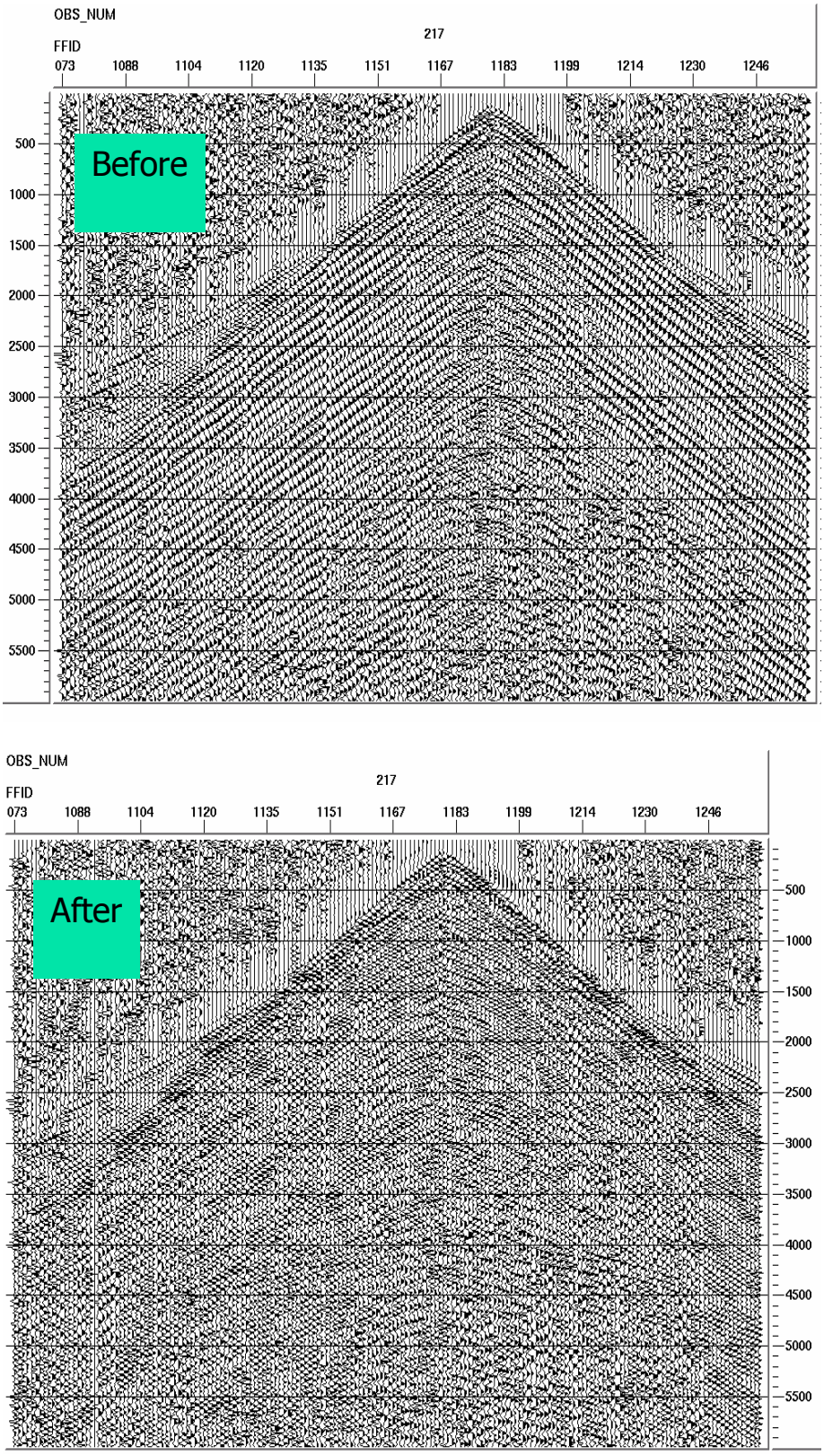

FIG. 16. Vertical component receiver gather before and after application of F-K filter to attenuate the reverberatory linear noise parallel to the first breaks.

ORIENTATION OF HORIZONTAL COMPONENTS

The geophone casing was gimballed so that the vertical component was known to be truly vertical on the sea floor. However, the azimuth of the horizontal components on the sea floor were unknown, so they needed to be determined from the data. The normal procedure would be to use an algorithm similar to the type that is used to orient 3C downhole geophones in VSP surveys. For example, simply rotating the horizontal components (in processing) to different azimuths, and measuring which azimuth yields the maximum energy on the radial, and minimum energy on the transverse components, is a commonly used method with 4C ocean-bottom data.

However, the differences in data quality between different horizontal components in this dataset, even on the same OBS instruments, made the entire procedure of combining components during processing difficult to do reliably. Standard procedures simply did not work properly at all. In the end it was determined that the most reliable method for determining the radial and transverse directions was to rotate the H1 and H2 components from -90° to 90° in increments of 30°, and then to choose the rotation which "looked best". The criteria for determining which angle looked best was that the magnitude and coherence of the first breaks and the reflections should look the strongest on the rotated H1 component when it is aligned with the direction that is radially outward from the shot to the receiver. This procedure was highly subjective, and ultimately not very reliable. However, it was the best that could be done with the available data.

It was impossible to determine whether shear-wave splitting was present in this data because of the irregularities in data quality and because of the problems in determining the orientation of the horizontal components, as described in the previous paragraph.

COMBINATION OF HYDROPHONE AND GEOPHONE DATA

The irregularities in the data quality between components also severely impacted the ability to attenuate multiples by combining hydrophone and geophone data. Ideally, OBS's on the ocean bottom provide an ideal, quiet recording environment, and potentially allows better multiple attenuation than streamer data because of the ability to remove receiver-side ghosts and receiver-side multiples by combining the hydrophone and geophone data. In a simplistic fashion this procedure requires only the estimation of a scalar, or short filter, which is applied to one component before adding the two datasets together.

Unfortunately in this case the estimation of this scalar value, or short filter, failed to be successful. The data irregularities essentially made it impossible to combine the hydrophone and geophone data in any way that led to an improved result. Figure 17 shows a typical result whereby the high-amplitude multiples from the hydrophone data and the high-frequency noise from the geophone are preserved in the combined data, thereby yielding the worst of both datasets.

The procedure that was ultimately followed was to process both the hydrophone and geophone datasets separately, and use Radon multiple attenuation to attempt to attenuate the multiples. Notice that the multiples in the vertical geophone data are far weaker than on the hydrophone data. This is exactly the result that is anticipated in an environment

that has a large sea floor reflection coefficient. As the reflection coefficient gets larger, the multiples naturally get weaker on the geophone data. So the need to combine the hydrophone and geophone data is reduced when the reflection coefficient is large since to a certain extent the geophone data will be "naturally" demultipled.

RADON MULTIPLE ATTENUATION

Figures 18, 19 and 20 show common-offset stacks before and after Radon multiple attenuation of the multiples below the base of Tertiary. An additional prestack F-K filter was applied after multiple attenuation, since the attenuation of the multiples revealed more linear noise that needed to be attenuated. The stacking velocities that were used for this data were obtained from the processing of some streamer data in the same location. This knowledge of stacking velocities greatly improved the performance of the Radon transform technique.

Notice that the amplitude of the primary event at the base of Tertiary at about 2150ms is much stronger after the multiples have been attenuated. However, notice the flat events at small offsets that are visible after multiple attenuation. These are probably artifacts due to imperfect separation of primaries and multiples in the Radon domain. Due to the flatness of these events, they will likely affect the final stacks.

In contrast, the multiples are clearly weaker to begin with on the vertical geophone component, and any artifacts that are generated at near offsets are certainly not as severe as for the hydrophone data. For this reason, it is anticipated that the vertical geophone data will provide a more accurate image below the base of Tertiary than the hydrophone component.

The radial component contains a relatively large amount of multiples below the base of Tertiary event at about 3750ms P-S time. As with the vertical geophone, a large amount of multiple energy was removed by the Radon method, but little primary energy appears to be present under the multiples.

STACKING, INTERPOLATION AND MIGRATION

Essentially one CDP line was obtained from each sail line shooting into the line of 21 receivers. Each of these lines comes from shot-receiver pairs with nearly constant crossline offset that is equal to the separation between the receiver line and the sail line. Figures 21, 22 and 23 show final CDP stacks of the inlines that are directly over the receiver line.

Since the spacing between sail lines is irregular (50m to 200m) there are irregular-sized gaps between each of the high-fold CDP lines. The data were sorted into 25m x 25m bins, which made the gaps anywhere from 1 to 3 bins wide. A crude method of eliminating the gaps would have been to use a wide CDP bin in the cross line direction. This would have led to a considerable amount of midpoint smear and only 12 bins in the corssline direction. A higher quality method of interpolation, such as f-xy interpolation, was not possible to apply because the spacing of live data lines is irregular, and because the width of the 3D is so narrow that it would not allow good enough statistics to be estimated in the crossline direction.

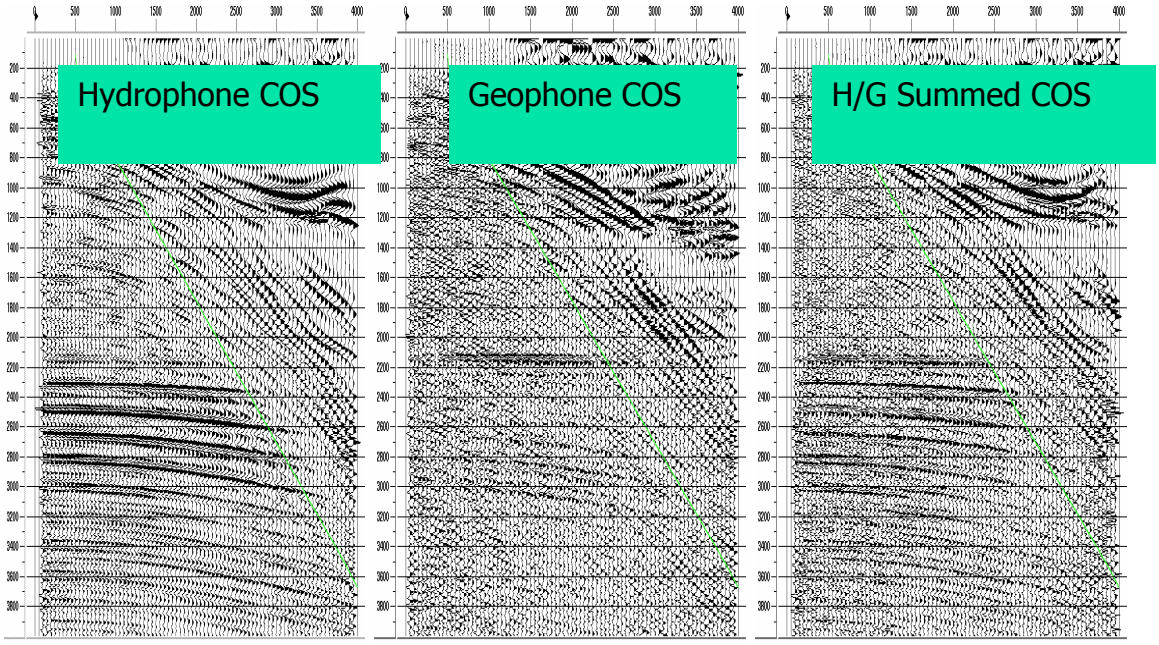

FIG. 17. Common-offset stacks of hydrophone, geophone, and combined hydrophone/ geophone data. Note that multiples have not been well attenuated in the combined data.

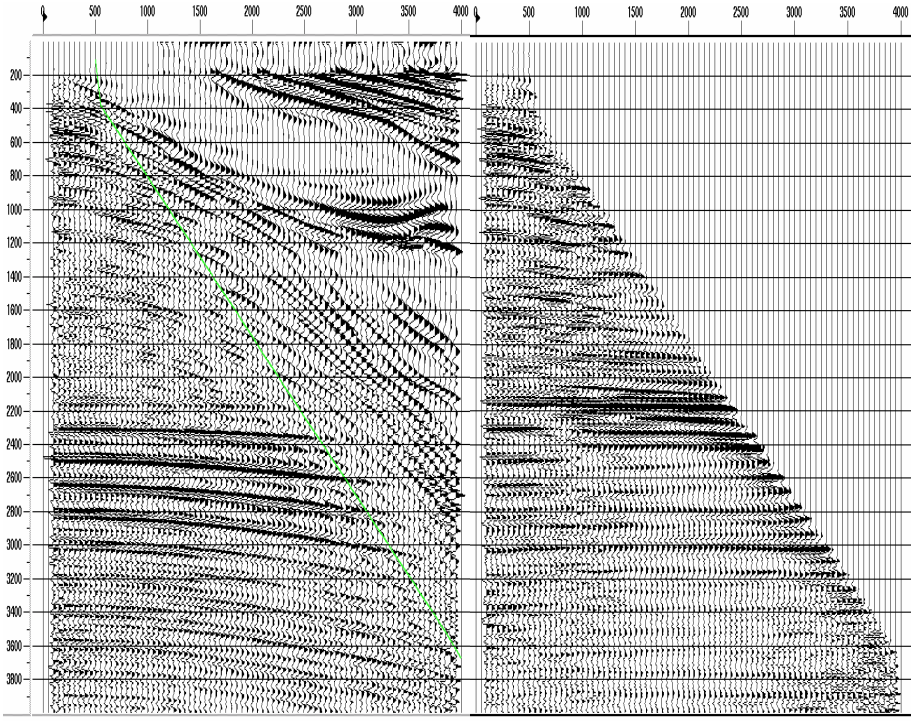

FIG. 18. Common-offset stack of hydrophone component before and after Radon and prestack F-K filters.

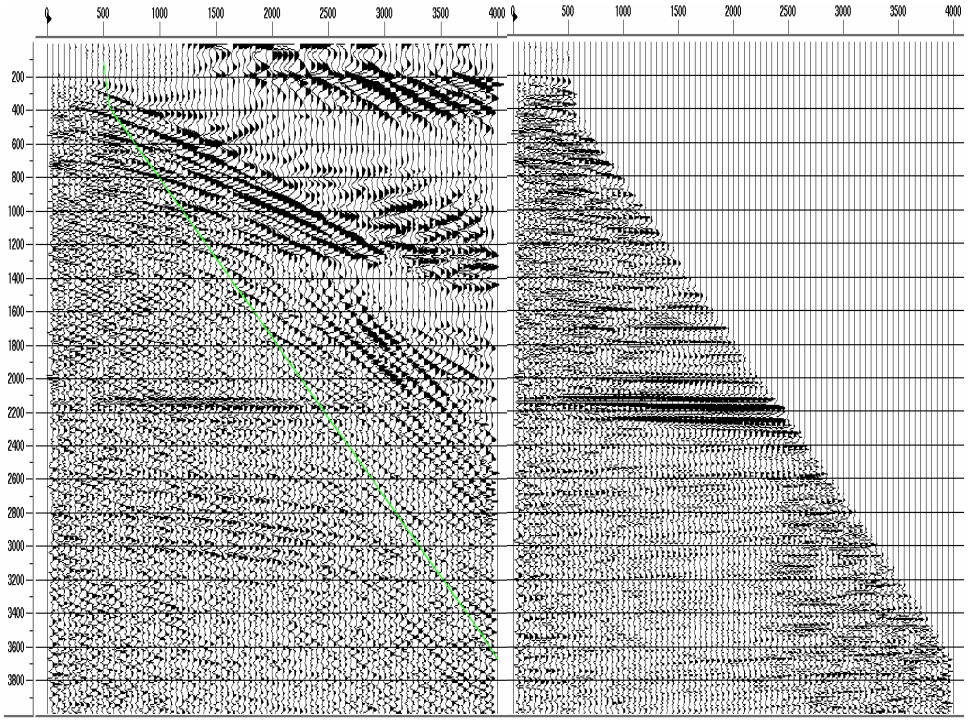

FIG. 19. Common-offset stack of vertical geophone component before and after Radon and prestack F-K filters.

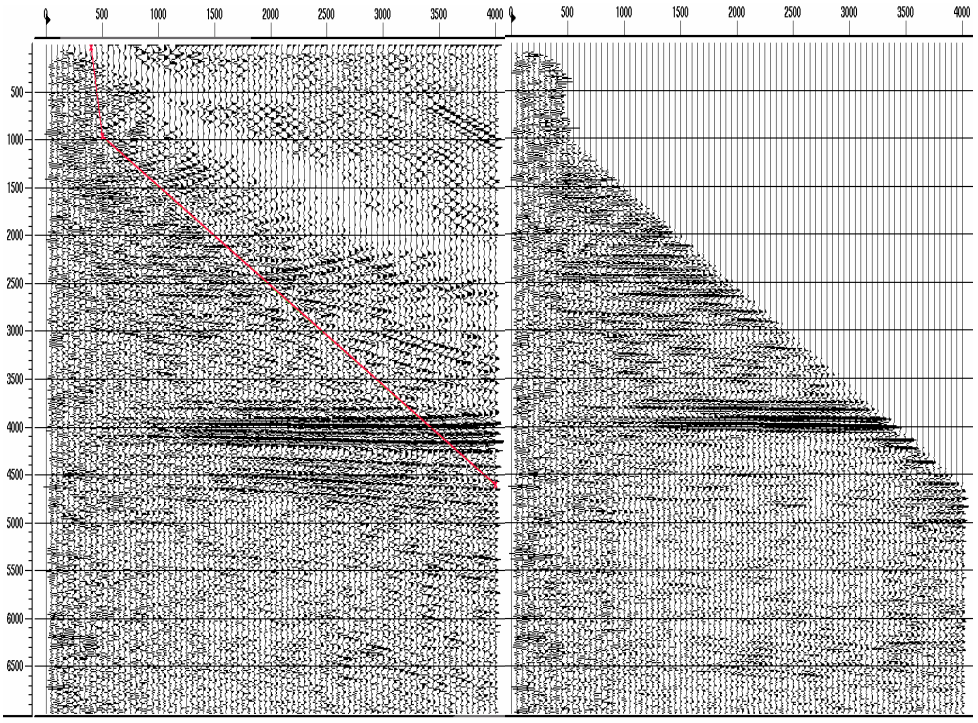

FIG. 20. Common-offset stack of radial geophone component before and after Radon and prestack F-K filters.

The method that was used to interpolate into empty bins was to use a sinc-function interpolation during the stacking of the data. The sinc function was made wide enough to smoothly interpolate from live bins into empty bins in the crossline direction. This method honours the true location of the midpoints but spreads the energy from each trace in the crossline direction as if the resolution in that direction is very poor (corresponding to a small maximum crossline wavenumber). It is similar to using a very wide bin width, but it still stacks the data in the right location. This method works best for flat events.

After interpolation, some poststack muting was performed around the edges and at the top of the volume, where the low fold did not allow a reasonable interpolation. Finally, the data were migrated using a standard finite-difference 3-D time migration. Figures 24, 25 and 26 show a selection of the migrated inlines.

RADIAL COMPONENT PROCESSING

The radial component was processed in a very similar way as the other components, with only a few exceptions. Shear wave statics were determined by aligning events within offset-limited receiver stacks. In normal converted-wave processing, more care would be taken during this process to ensure that structure is not being altered. Given the questionable reliability of the other components, however, preservation of structure could not be guaranteed in this case. The statics method that was used was focused more on simply extracting coherent events from the data, not on preserving their structural dip.

Deconvolution, residual statics, and velocity analysis were done in the same way as for the hydrophone and vertical geophone. The data were asymptotically binned and depth-variant binned during stacking using a constant Vp/Vs of 2.05. The vertical Vp/Vs is known from a well within the survey area to vary from values above 3.0 in the shallow section, to about 2.0 at the base of Tertiary. Below the base of the Tertiary the values are in the 1.7 to 1.8 range. The average value of vertical Vp/Vs at the base of Tertiary is about 2.85. A much smaller Vp/Vs of 2.05 was used to bin the data since the effective Vp/Vs (a combination of vertical and stacking Vp/Vs) is what controls the position of the conversion point. From processing in other areas, it is common to find that the effective Vp/Vs is about 60% to 70% of the vertical Vp/Vs. This is why such a low value of Vp/Vs was used for binning. The value of 2.05 was used instead of a round number like 2.00 only because 2.05 yields a more regular distribution of conversion points within bins.

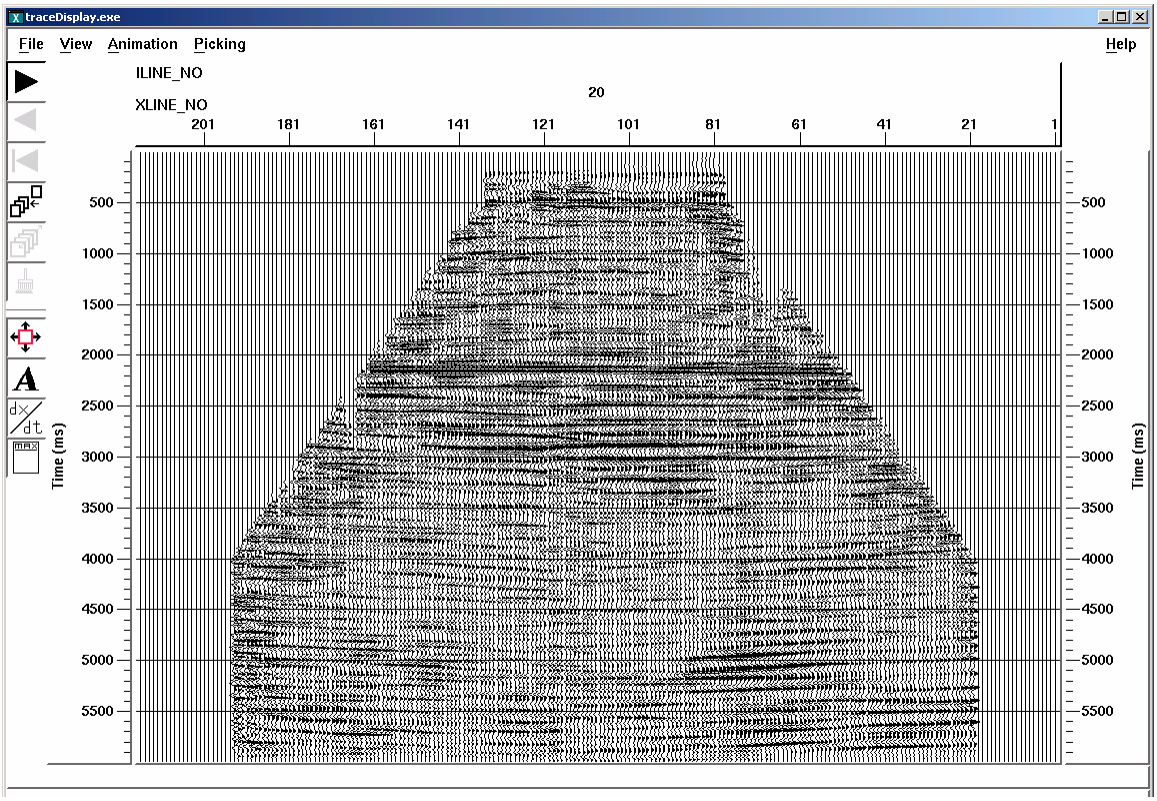

FIG. 21. Central inline from final stack of hydrophone component.

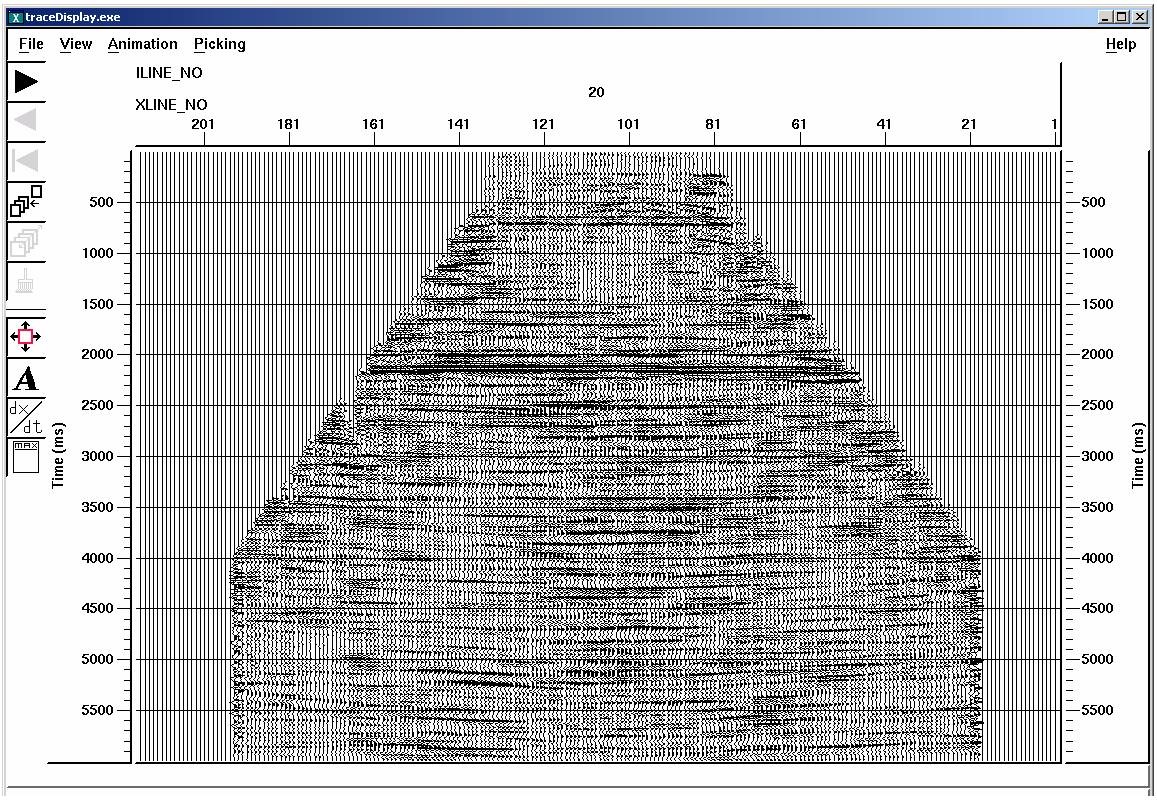

FIG. 22. Central inline from final stack of vertical geophone component.

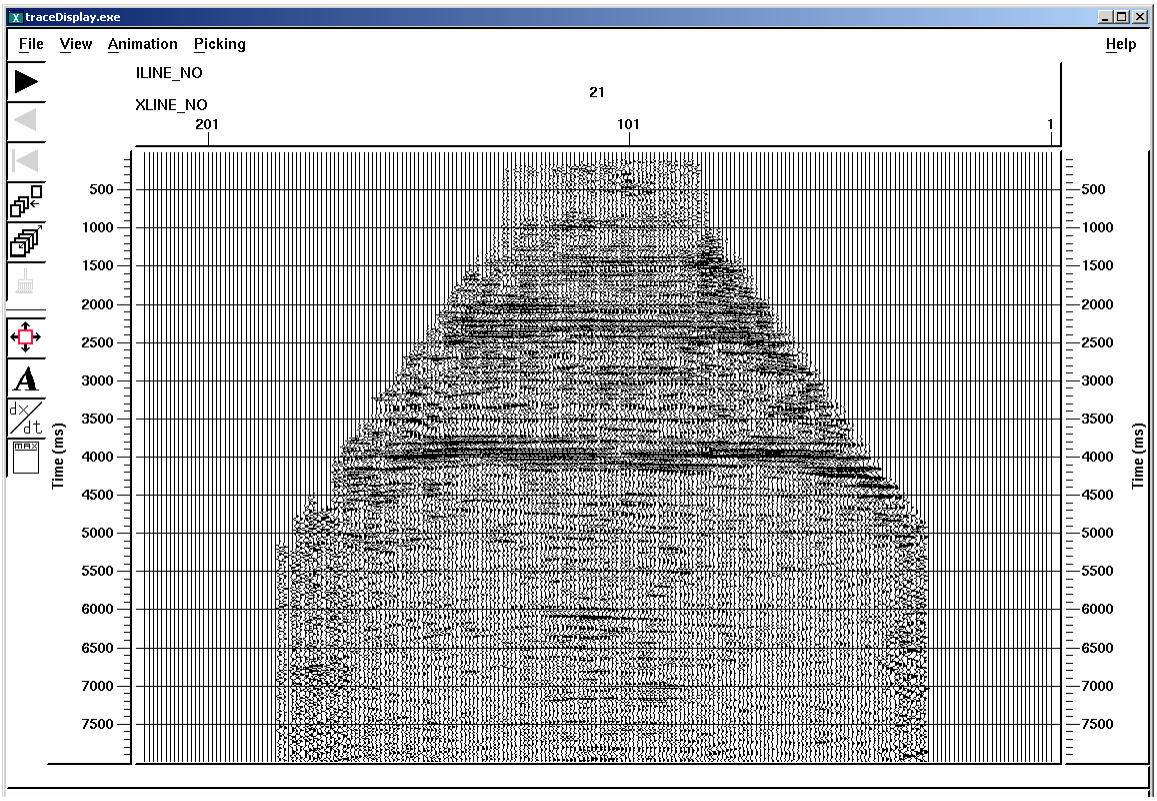

FIG. 23. Central inline from final stack of radial geophone component.

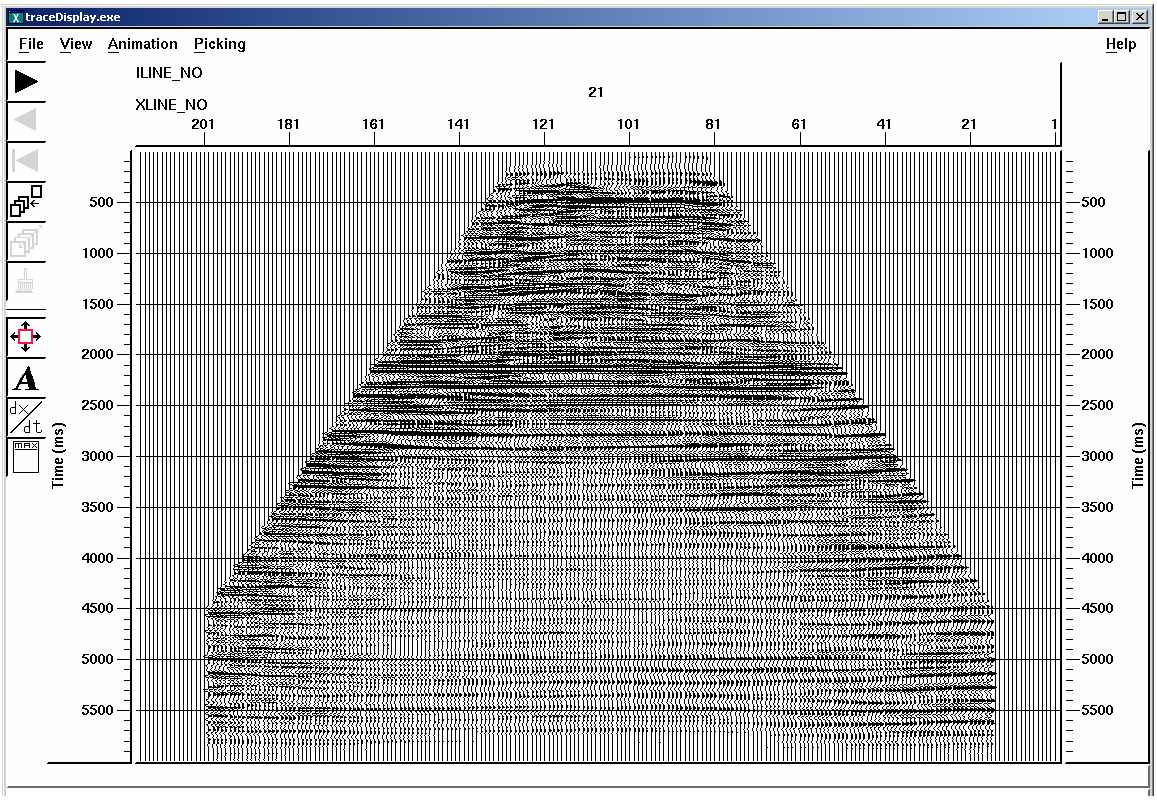

FIG. 24. Central inline from migrated stack of hydrophone component.

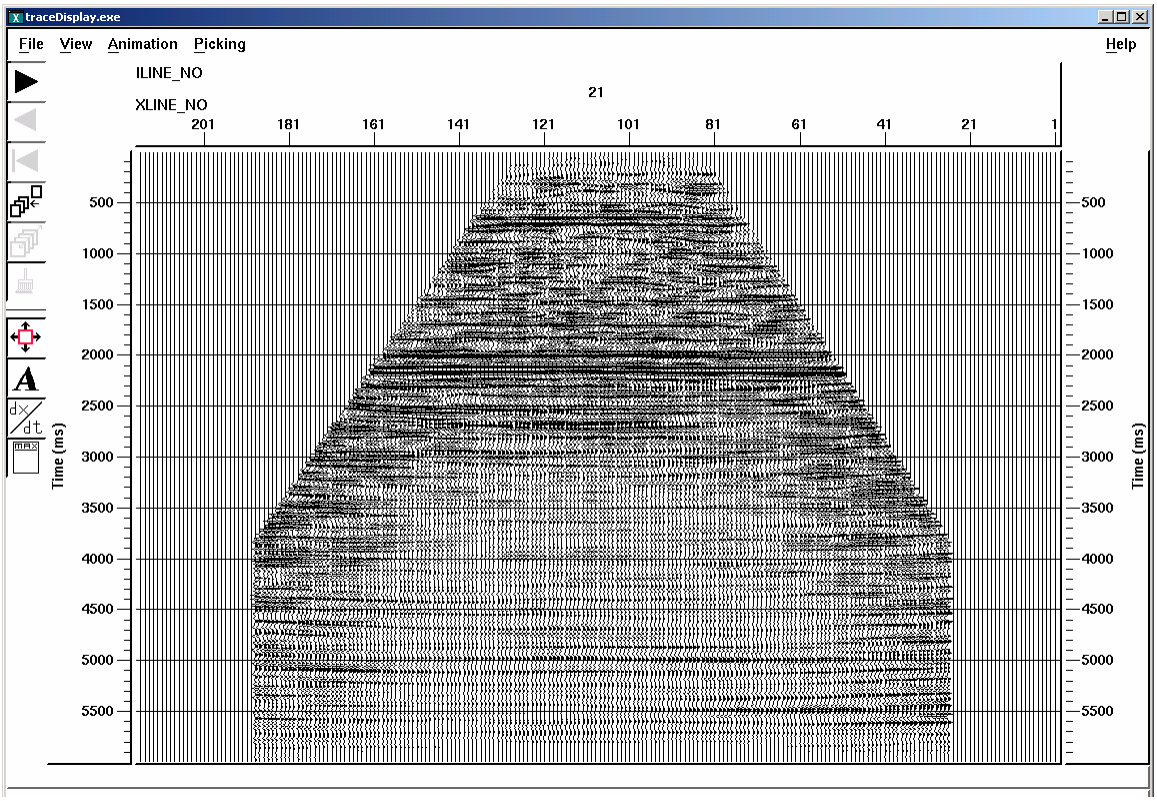

FIG. 25. Central inline from migrated stack of vertical geophone component.

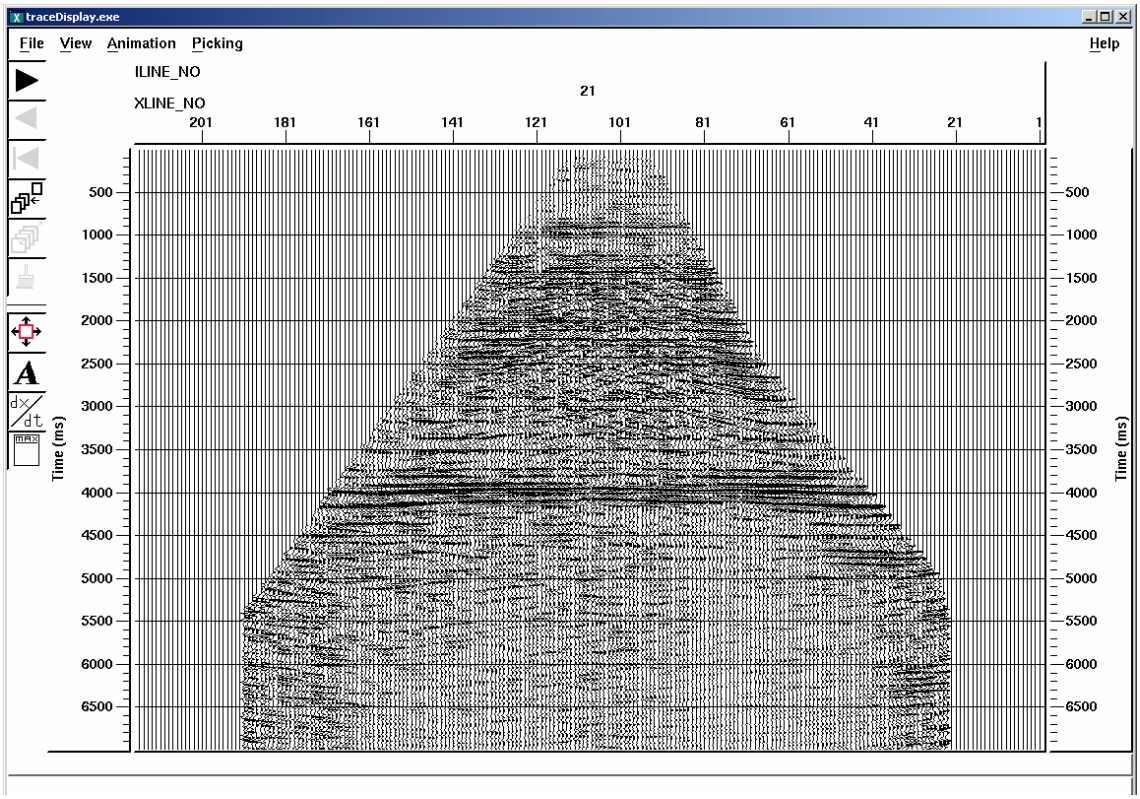

FIG. 26. Central inline from migrated stack of radial geophone component

CONCLUSIONS

Given the many problems with the quality of the data that was recorded, it was remarkable that the coherence of the events in the final migrated sections is so good. The problems with the data did severely hamper the processing efforts.

In particular, steps such as the combination of the hydrophone and geophone records to attenuate multiples, and the rotation of the horizontal components into radial and transverse coordinates could not be performed with reliability. The multiples on the hydrophone component are so strong that it is doubtful that the Radon filter that was used to attenuate them was entirely successful. On the other hand, the coherent events on the vertical geophone component are likely to be real since the multiples affected that component much less than the hydrophone. Coherent events were imaged on the radial component, but some of the processing steps such as rotating into the radial direction were not done with much confidence of their correctness. The reflectors below the base of Tertiary are known to have a fair amount of time structure, which does not appear on these final stacks. Unfortunately some of the structural elements in this data may have been lost in the processing in attempts to simply obtain any coherent events below the base of Tertiary.

Ultimately, this was an extremely useful test since it proved that high-quality multicomponent images can be obtained from this area with improvements in the instrumentation.